

Doppler-free nonlinear absorption in ethylene by use of continuous-wave cavity ringdown spectroscopy

Christine R. Bucher, Kevin K. Lehmann, David F. Plusquellic, and Gerald T. Fraser

We report what we believe to be the first systematic study of Doppler-free, nonlinear absorption by use of cavity ringdown spectroscopy. We have developed a variant of cavity ringdown spectroscopy for the mid-infrared region between 9 and 11 μm , exploiting the intracavity power buildup that is possible with continuous-wave lasers. The infrared source consists of a continuous-wave CO_2 laser with 1-mW tunable infrared sidebands that couple into a high-finesse stable resonator. We tune the sideband frequencies to observe a saturated, Doppler-free Lamb dip in the ν_7 , $11_{1,10} \leftarrow 11_{2,10}$ rovibrational transition of ethylene (C_2H_4). Power studies of the Lamb dip are presented to examine the intracavity effects of saturation on the Lamb-dip linewidth, the peak depth, and the broadband absorption. © 2000 Optical Society of America

OCIS codes: 230.5750, 300.6190, 300.6320, 300.6340, 300.6420, 300.6460.

1. Introduction

Cavity ringdown spectroscopy (CRDS) is a technique developed for the observation of weak absorption signals. The principles of CRDS are quite simple. Light couples into a high-finesse optical cavity, known as a ringdown cavity, defined by two highly reflective mirrors that propagate back and forth inside the cavity. The highly reflective mirrors effectively lengthen the absorption path length, and propagation path lengths can reach from 10^2 to 10^5 times the cavity length. On each pass through the ringdown cavity, the light experiences a small intensity loss that is due to the <100% mirror reflectivity and absorption by the sample contained between the mirrors. One can observe the total optical loss of the cavity by monitoring the free (i.e., without driving radiation) decay of the energy stored in the cavity.

When this research was performed, C. R. Bucher and K. K. Lehmann (lehmann@princeton.edu) were with the Department of Chemistry, Princeton University, Princeton, New Jersey 08544. C. R. Bucher (christine.bucher@mpq.mpg.de) is now with the Laser Chemistry Division, Max-Planck-Institute for Quantum Optics, Max-Planck-Gesellschaft, Hans-Kopfermann Strasse 1, 85740 Garching, Germany. D. F. Plusquellic (dplus@nist.gov) and G. T. Fraser are with the Optical Technology Division, National Institute of Standards and Technology, Gaithersburg, Maryland 20899-8441.

Received 2 July 1999; revised manuscript received 22 December 1999.

0003-6935/00/183154-11\$15.00/0

© 2000 Optical Society of America

For linear absorption and when the optical loss is constant for all optical frequencies coupled into the cavity, the time-varying intensity decay is exponential, and the ringdown decay rate, $k(\omega)$, is a measure of the total loss inside the cavity. The characteristic ringdown decay rate is represented by the following equation:

$$k(\omega) = 2(1 - R)/t_r + c\alpha(\omega), \quad (1)$$

where R is the mirror power reflectivity, $t_r = 2L/c$ is the optical round-trip time of the cavity, L is the cavity length, ω is the angular frequency of the radiation, c is the speed of light, and $\alpha(\omega)$ is the absorption coefficient of the medium contained between the mirrors. For an empty cavity we determined the ringdown rate by L and R , where R is assumed to change slowly with frequency. If an absorbing species is introduced into the cavity, the ringdown rate increases by $c\alpha(\omega)$ because of the additional loss term. Therefore, CRDS measures absorption as the change in the rate of light intensity decay inside a high-finesse optical cavity, and several papers discuss the linear response theory of CRDS more rigorously.¹⁻⁴ This theory is identical for excitation of a ringdown cavity by both pulsed and continuous-wave (cw) lasers although experimental subtleties exist to implement the two approaches.

The majority of CRDS experiments reported to date have used nanosecond pulsed laser sources. For example, O'Keefe and Deacon first demonstrated the sensitivity of CRDS by using a nanosecond pulsed

dye laser to observe the highly forbidden atmospheric bands of O₂.⁵ However, pulsed lasers produce certain limitations on CRDS performance, which are surmountable through the use of cw lasers. For this reason, there has been an increased interest in employing cw lasers for CRDS measurements.⁶⁻⁸ The first cw CRDS experiments were carried out at Princeton,⁹ but the first successful implementation was reported by Romanini *et al.*¹⁰ Engeln *et al.*⁸ introduced a phase-shift, cavity ringdown method, but this method does not involve measurement of the cavity decay.¹¹ There are several advantages of cw CRDS as have been discussed in Refs. 10 and 12-14. The primary advantage is that a single mode of the ringdown cavity can be excited with a narrow-bandwidth cw laser. When the laser is tuned to one of the cavity resonances, intracavity intensity buildup results. In addition, more light can couple into the ringdown cavity with cw excitation because of the improved spectral overlap between the laser linewidth and the cavity mode width. Therefore, when one uses cw lasers, the intracavity light intensity can be several orders of magnitude larger than the excitation source whereas in traditional pulsed-excitation experiments, the intracavity intensity is many orders of magnitude smaller than the source. Thus, the two excitation methods can result in similar intracavity power even when the peak power of the pulsed source is $\sim 10^9$ times larger. In the cw regime, then, the cavity enhances the possibility of the observation of nonlinear effects as a result of the intracavity power buildup. Even with low-power lasers, saturated absorption by use of CRDS becomes feasible, and nonlinear spectroscopy opens up many new possibilities. Despite this, we know of only one report on nonlinear optical effects observed by CRDS. Romanini *et al.*¹⁵ observed nonlinear optical effects in the electronic spectrum of NO₂ near 796 nm, including saturation, Lamb dips, and two-photon excitation (observed in fluorescence). However, we do not present any quantitative study of these effects.

Besides developing cw CRDS techniques, another general motivation is to expand the wavelength region covered by CRDS. The mid-infrared region is appealing for the extension of CRDS because it effectively ensures that all polyatomic molecules have rovibrational transitions in this spectral range. However, this region originally received little interest because of the lack of highly reflective mirrors for these wavelengths. The first CRDS studies in the infrared were reported by Scherer *et al.*¹⁶ at 1.6 and 3.3 μm . Mid-infrared CRDS studies have been reported by three groups working in the 8-11- μm region. By using a free-electron laser, Engeln and co-workers measured ethylene spectra with a standard CRD detection scheme and also by a Fourier-transform multiplex detection method.¹⁷ Crosson *et al.* used a synch pumping or pulse-stacking excitation scheme, in which many pulses from a free-electron laser are coherently added by making n times the ringdown cavity rate equal to the pulse repetition rate of the free-electron laser, leading to dramatic

increases in optical throughput.¹⁸ Muertz and co-workers studied ethylene trace-gas absorption with a line-tunable CO₂ laser and compared their results with photoacoustic measurements.¹⁹ For this study we used a laser setup that is similar to that used by Muertz *et al.*, but we adapted it to provide greater tunability and optimized it to obtain orders-of-magnitude higher sensitivity.

We developed a novel variant of cw CRDS for the mid-infrared region between 9 and 11 μm by exploiting the intracavity power buildup that is possible with cw CRDS to observe nonlinear absorption. A cw CO₂ laser system with tunable infrared sidebands couples into a ringdown cavity and produces a saturated absorption in an inhomogeneously broadened rovibrational line of ethylene. The cavity is closely locked to one of the sidebands, allowing for >200 -fold enhancement of the intracavity power over the source. To our knowledge we report the first systematic study of Doppler-free nonlinear absorption by use of cw CRDS. Power studies on the absorption, measured by CRDS, are presented to understand the effect of saturation on the Lamb-dip linewidth, peak height, and broadband absorption. A potential application of these saturation measurements is that, when they are considered along with the intracavity electric field, the transition dipole moment for a sample can be calculated without prior knowledge of the concentration. This technique, thus, holds great promise for IR measurements of transient or unstable species.

2. Experimental

Figure 1 is a schematic of the experimental optical setup. The principal components are a line-tunable CO₂ laser, a microwave synthesizer and amplifier, a CdTe electro-optic modulator (EOM), a 1.12-m-long vacuum-sealed cavity for the ringdown measurements, and a stabilized reference cavity and spectrum analyzer for frequency stabilization and calibration of the laser source. The CO₂ laser generates as much as 10 W of infrared radiation with a short-term (~ 1 s) instrumental linewidth of 180-kHz (peak-to-peak after locking). One can generate tunable infrared sidebands ($\Delta\nu = 12$ -18 GHz) on the CO₂ carrier by mixing 20 W of amplified microwave power with the infrared radiation in the EOM.²⁰ The two infrared sidebands emerge from the EOM with orthogonal polarization to the CO₂ carrier and with a power of ~ 1 mW in each. A p-i-n diode switch²¹ in front of the microwave amplifier provides a fast gate (rise time of ~ 10 ns) for on and off intensity modulation of the sideband power at a repetition rate of 15 kHz. A Ge wedge oriented at the Brewster angle separates the S-polarized sideband frequencies from the P-polarized carrier frequency with an efficiency of $\sim 100:1$. The reflected sideband light couples into the ringdown cavity after encountering two ZnSe lenses that are optimized for mode matching into the TEM₀₀ mode of the cavity. Only one sideband is generally transmitted by the cavity inasmuch as the cavity functions as a frequency filter. Further fre-

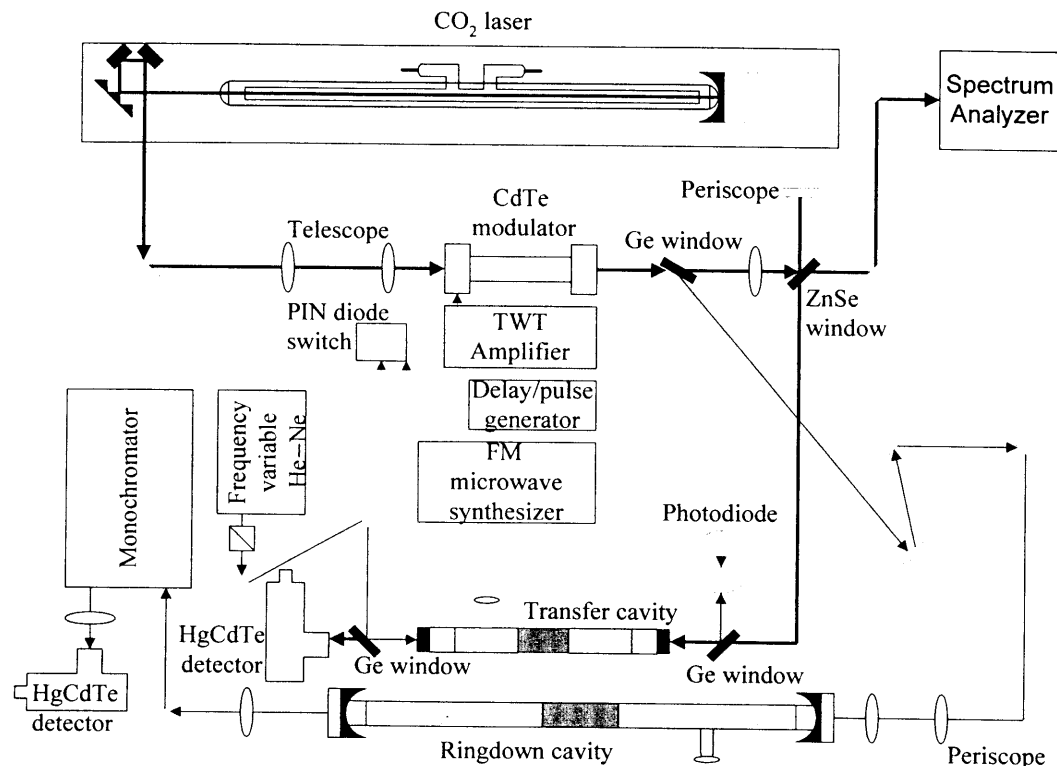


Fig. 1. Optical experimental setup. TWT, traveling-wave tube.

frequency discrimination occurs with a monochromator (0.75 m with $f/8$ optics and entrance and exit slit widths of 200 and 100 μm , respectively) to provide for a clean spectral separation of one sideband from the residual carrier and the other sideband. The infrared light is focused ($F = 2.54$ cm) onto a liquid-nitrogen-cooled HgCdTe detector with an 80-ns rise time (this rise time is measured and represents the convolution of the detector and the infrared intensity modulation) and a 400- μs high-pass response.

A. Ringdown Cavity

The ringdown cavity (noncommercial) consists of a near-confocal Fabry-Perot resonator constructed from a hollow Pyrex tube (1.12 m long and 2.54-cm outer diameter) with a stainless-steel central section (~ 0.3 m). Heating tape is wrapped around the stainless-steel area for cavity-length control. At either end of the cavity is a 2.54-cm-long piezoelectric transducer (PZT) to which a ZnSe mirror is attached. The two concave mirrors have a 1-m radius of curvature and a coating of $R = 99.5\%$ reflectivity at 10.6 μm .²² The mirrors are held in aluminum plates that screw into Maycor cavity end pieces. Compression of the mirrors against O rings in the Maycor end pieces creates the vacuum seal.

From the cavity geometry and mirror curvature, a round-trip time of 7.47 ns, a longitudinal-mode separation of 134 MHz, and a transverse-mode spacing of 72 MHz are calculated. At 10.6 μm , the TEM_{00} mode of the cavity has a beam waist of 1.03 mm at the center and 2.0 mm at the mirrors. The Fresnel

number of the cavity is calculated to be 52, implying that diffraction losses are completely negligible for the lower-order transverse modes. The measured ringdown time t of the evacuated cavity is 736 ns from which $R = 99.49\%$ can be calculated, implying that each cavity mode has a linewidth of 216-kHz FWHM and the cavity has a finesse of 617. The effective path length ct of the cell is 225 m. We performed optical alignment and telescope adjustments by rapidly sweeping the sideband frequency and/or the PZT voltage over a free spectral range of the cavity and by observing the transmitted light intensity. Both to maximize sensitivity and to allow for calculation of the modal distribution inside the cavity, it is important for one to ensure that only the TEM_{00} mode of the cavity is excited. The nearest low-order coincidence of cavity modes has a separation of 10 MHz, which is much greater than the linewidths of both the cavity modes and the laser. Thus, excitation of a pure TEM_{00} mode is expected if the peak of this mode is locked to the laser frequency.

The cavity length is adjusted through the use of the two PZT's at each end of the cavity and the heated stainless-steel central section. The cavity is made of Pyrex for electrical isolation of these elements. A high-voltage amplifier (~ 4 kV) drives the PZT's for fast changes (>200 Hz) in cavity length with a tuning range that is slightly greater than a free spectral range at 10.6 μm . Slower temperature-induced length changes of the heated stainless-steel section provide for coarse adjustment of the mirror separation over many optical wavelengths. The ringdown

cavity length is actively locked to maintain resonance of a TEM₀₀ mode with one of the sidebands of the CO₂ laser. The sideband frequency is modulated at 100 kHz with a modulation depth of 20 kHz and the demodulated error signal is first conditioned in proportional, integral, and differential (PID) gain stages and then used to regulate both the voltage to the PZT amplifier and the current to the heater tape. Based on the magnitude of the error signal and the 216-kHz linewidth (FWHM) of the evacuated cavity, the lock stability is estimated to be better than 100-kHz (peak-to-peak) over a period of hours, as determined by the residual feedback signal. It is also noted that this lock is not significantly degraded despite the 100% modulation of the sideband power needed to observe the ringdown transients. An estimate of the short-term stability during the 22- μ s ringdown periods is \sim 100 kHz based on the transient response of the error signal at the moment the sideband is switched back on.

B. CO₂ Laser Calibration and Stabilization

The CO₂ laser system has been described previously.²³ We identified the CO₂ laser lines by using a spectrum analyzer. For more precise frequency control, a He-Ne-stabilized transfer cavity²⁴ is used to stabilize actively the CO₂ laser frequency. The transfer cavity is 53 cm long with a cavity spacer that is identical in design to the ringdown cell. The ZnSe mirrors have a double-V dielectric coating for reflectivity at both 0.632 and 10.6 μ m and radii of curvature of 1 m, which creates nondegenerate cavity modes and 283-MHz free spectral range of the TEM₀₀ modes. The cavity is also evacuated to eliminate the effects of dispersion that are due to ambient pressure changes. We combined and separated the He-Ne and the CO₂ lasers by using dichroic optics, and we detected cavity transmission signals by using a silicon photodiode and a liquid-nitrogen-cooled HgCdTe detector, respectively. Lock-in methods first stabilized the transfer cavity to the He-Ne laser and then the CO₂ laser frequency to the transfer cavity. Inasmuch as both lasers share a common cavity, it is convenient to dither the spacer length (\sim 4 kHz), which gives modulated transmission signals near cavity resonances at both colors. However, the two frequencies differ by 17 fold, and thus the modulation depths (in megahertz) for the two colors differ by the same factor. To maximize the signal-to-noise ratios for the lock-in methods, it is desirable to have similar modulation amplitudes at both colors for a given change in cavity length. We accomplished this by making the mirror reflectivities $<70\%$ and 98.5% at 0.632 and 10.6 μ m, respectively. As before, the demodulated signals are conditioned in proportional and integral gain stages that are used to regulate the PZT high voltage and heater current to the transfer cavity and the high voltage to the PZT-controlled end mirror of the CO₂ laser cavity. Tunability of the He-Ne frequency in combination with access to higher-order modes of the nondegenerate cavity permit lock-point selection at any CO₂ laser frequency.

The long-term stability of the He-Ne laser is estimated to be 1.5 MHz, which implies a stability of the CO₂ laser of <125 kHz. The drift of the sideband radiation matches that of the CO₂ carrier, since the microwave source has a negligible frequency drift on this scale. The CO₂ laser stability is comparable with the calculated transit-time broadening in this experiment, and the <125 -kHz long-term stability of the CO₂ sideband has been confirmed in repeated Lamb-dip measurements made over a period of many hours.

C. Signal Acquisition and Averaging

Individual ringdown curves are digitized at a sampling rate of 20 MHz over a period of 5 μ s by use of a digital oscilloscope with 8 bits of vertical resolution. Thus, each recorded ringdown transient contains 100 points that extends over more than six time constants of the decay. After 44 μ s, the sideband power is switched back on for 22 μ s. A fixed number of decay transients, typically 100, are averaged in the transient digitizer (LeCroy 9350M) and are then transferred to a personal computer where the transient is fit to a first-order exponential function by use of a nonlinear least-squares procedure. The best-fit decay time t is saved as a function of sideband frequency at stepped intervals of 100 kHz or less. The 15-kHz ringdown transient detection rate is limited by the digitizer.

Inasmuch as the degree of optical saturation depends on the intracavity power, a method to stabilize the optical power in the cavity is employed that takes advantage of the rapid feedback control of the applied microwave power. Two gates are positioned at different times along the detector signal. One gate monitors the detector signal prior to switching off the sideband radiation, and the other gate monitors the detector signal prior to switching on the sideband radiation. Each gate integrates at 1- μ s intervals along the detector voltage. The signals from the two gates are then sent to boxcars and subtracted, and the voltage difference is used to regulate the applied microwave power on a shot-to-shot basis. Power-level variations over the course of a scan are typically better than 0.5%. We also note that the intracavity loss, and thus the Q of the resonator, changes with frequency when one tunes through a transition. At a fixed output power level, the intracavity power is effectively constant as well, requiring that the input power be increased at frequencies for which the cavity loss increases. Measurement error is currently limited by systematic variations in the ringdown times; however, potential nonlinearity of the detector cannot be fully discounted. Power leveling reduces the systematic error by more than tenfold, decreasing rms fluctuations in the fitted ringdown rates to 0.085% (for 400 fits with an average of 100 decays per fit).

A premixed sample containing $0.5\% \pm 0.05\%$ of C₂H₄ in He (by volume) continuously flows through the cavity at a total pressure of 1.3 ± 0.3 Pa, yielding a number density of 1.6×10^{12} cm⁻³. A 1.3-kPa

obtained in this study. It can be seen that, prior to the observation of the ringdown transient, the intracavity light intensity is constant for a time long compared with the relaxation times, and thus a steady state should be achieved. However, the ringdown time is short compared with the relaxation times, so it should be a reasonable assumption that the molecular absorption coefficient remains constant at the saturated value predicted by the intracavity intensity at the beginning of the ringdown decay.

When we make a comparison with our experimental results, we must consider the fact that the optical transition is not a single two-level system, but a series of degenerate transitions. This results from the fact that the transition dipole depends on the value of the projection of the angular momentum on the axis of polarization of the laser beam and is in fact linear with M for a Q -branch transition, as considered here. We can thus write

$$\mu_{12}(M) = \mu_0 M / [J(J+1)]^{1/2}. \quad (3)$$

The fractional population of the lower state of the transition is calculated to be 3.2×10^{-3} . Combined with the integrated line intensity, a value of $\mu_0 = 1.01 \times 10^{-30}$ C m (0.305 D) was calculated. In addition to the inhomogeneous distribution of transition moments, there is a distribution of the closest point of approach of the molecules to the optical axis, the velocity at which they move through the field, and also where they are at the start of the ringdown decay.

In steady state and assuming that the optical Bloch equations are valid, the degree of saturation in the Doppler-broadened line is determined by the saturation parameter S . It is related to the saturating electric field E and the transition dipole moment μ_{12} by the following equation:

$$S = [\mu_{12}E/\hbar]^2 T_1 T_2, \quad (4)$$

where T_1 is the population relaxation lifetime (assumed to be the same for the upper and lower states of the transition) and T_2 is the homogeneous dephasing time.³¹ Under the low-pressure conditions of the present experiment, both T_1 and T_2 are expected to be equal and determined by transit-time broadening T_t , produced by the thermal motion of the absorbers through the laser field. Given the mean speed transverse to the laser propagation direction of $v = 421$ m/s for C_2H_4 and a TEM₀₀ spot size of $w_0 = 1.03$ mm, T_t is calculated to be $w_0/v = 2.3$ μ s.³² Transit-time broadening produces a Gaussian homogeneous line shape (ignoring the spread of transverse velocity) with a FWHM given by $0.37/T_t = 155$ kHz (for a complete theory of the saturated line shape, see Ref. 33). This calculation holds for the beam waist, but as one moves away from the center of the cavity, the spot size increases (decreasing the transit-time broadening), and the beam develops a curvature, leading to homogeneous Doppler broadening at low power. The two effects cancel for a TEM₀₀ mode so that the homogeneous line shape is the same throughout the cavity.³³ An inconsistency in the present treatment is

that the optical Bloch equations predict a Lorentzian homogeneous line shape.

The saturation parameter can also be expressed in terms of intensity so that Eq. (4) can be rewritten as $S = I/I_S$, where intracavity intensity I is related to the electric field by

$$I = E^2 c \epsilon / 2, \quad (5)$$

and saturation intensity I_S is given by

$$I_S = \hbar^2 c \epsilon / 2 \mu_{12}^2 T_1 T_2. \quad (6)$$

The saturation parameter is expected to be linearly proportional to the electric field intensity within the resonator and is therefore proportional to resonator output power. Away from the Lamb dip, the relevant intensity is the one-way power, inasmuch as the forward and the backward waves in the cavity are in resonance with separate velocity classes of molecule. On the peak of the Lamb dip, both the forward and the backward waves couple to the same velocity class of molecules, and thus the saturation parameter is approximately doubled.³⁴ By increasing the saturating power, the nonlinear effect becomes more pronounced.

Figure 4 shows the influence of saturation on the Lamb dip for three different saturation powers. In this experiment, we controlled the saturation power by changing the microwave power that couples into the EOM and hence determines the power in the IR sideband. Larger ringdown amplitudes correspond to greater saturation powers, inasmuch as the transmitted power is proportional to the intracavity power. As the power of the saturating beam increases, three saturation effects result: the Lamb-dip linewidth broadens, the baseline absorption rate away from the Lamb dip decreases, and the dip depth decreases.

These effects are predicted for optical saturation of a two-level system in steady state and are related to saturation parameter S . The Lamb-dip linewidth is the homogeneous linewidth at low power times a saturation factor, i.e. the homogeneous linewidth is power broadened:

$$\Delta v_S = \Delta v_H (1 + S)^{1/2}, \quad (7)$$

where Δv_H is the homogeneous linewidth of the transition. The line shape of the Lamb dip when coherent effects are neglected is expressed by³¹

$$\alpha_M(\nu) = \alpha_{EC} + \alpha_0(\nu) \frac{\Delta v_H/2}{B \left\{ 1 - \left[\frac{2(\nu - \nu_0)}{A + B} \right]^2 \right\}^{1/2}}, \quad (8a)$$

with

$$A = [(\nu - \nu_0)^2 + (\Delta v_H/2)^2]^{1/2}, \\ B = [(\nu - \nu_0)^2 + (\Delta v_H/2)^2 (1 + 2S)]^{1/2} \quad (8b)$$

$$\alpha_0(\nu) = \alpha_0 \exp \left[-2 \ln 4 \frac{(\nu - \nu_0)^2}{\Delta v_D^2} \right], \quad (8c)$$

where $\alpha_M(v)$ is the measured absorption rate, α_0 is the unsaturated absorption coefficient, ν_0 is the absorption center frequency, and $\Delta\nu_D$ is the room-temperature Doppler width fixed at 66.5 MHz. In Eq. (8a) we have also included the empty-cavity ring-down rate, α_{EC} , for the purposes of fitting our data. It is easily verified that for $S = 0$ Eqs. (8) reduce to the sum of the rates, $\alpha_0(v)$ and α_{EC} , expected in the linear absorption limit. For frequencies away from the absorption center, the decrease in the broadband optical absorption with saturation is given by a reduction of Eq. (8a):

$$\alpha_S(v) = \alpha_0(v)/(1 + S)^{1/2}. \quad (9)$$

Dip depth D depends on S according to the following equation:

$$D = \alpha_0[1/(1 + S)^{1/2} - 1/(1 + 2S)^{1/2}]. \quad (10)$$

Our initial interest is to apply this simple theory to the CRD data of ethylene to determine if it can account for the effects of saturation on a system for which all the parameters in Eqs. (8) are known except for S . The homogeneous linewidth, $\Delta\nu_H$, is fixed at 0.155 MHz and is determined from transit time broadening because this broadening dominates at low power. In the top panel of Fig. 4, we show the line shapes predicted (dashed curves) from nonlinear least-squares fits of the data to Eqs. (8) for three different intracavity powers. The empty-cavity ringdown rate, α_{EC} , and the unsaturated absorption coefficient, α_0 , are fixed at 1.358 and 0.811 MHz, respectively. For the Lamb dips acquired at relative powers of 2.0 and 3.6 (lower two traces), the predicted curves are only a poor representation of the observed line shapes. The best-fit values of saturation parameter S are shown at left in Fig. 4. For the lowest intracavity power (top trace), the model fails completely; it is not possible to fit S within these parameter constraints because the observed absorption rates of the dip exceed those predicted for linear absorption with $S = 0$ (dashed curve). To verify that the sample concentration is not the source of this discrepancy, we made an independent direct absorption measurement of the gas by using a Fourier-transform infrared spectrometer with a 10-cm absorption path length and found that the concentration is identical to our initial measurement taken with the literature value for the line strength,²⁶ thus confirming the unsaturated absorption rate of 0.811 MHz.

To provide further insight into the model's failure to account for the observed trends, we refit the data to Eqs. (8) by relaxing the constraints on α_{EC} and α_0 . A summary of the fitted parameters and uncertainties is given in Table 1, in which Type A standard uncertainties (i.e., 1σ) are given, as determined directly from the least-squares fit. The predicted line shapes are shown as dashed curves in the lower panel of Fig. 4 and are now in good agreement with experiment. However, the empty-cavity decay rates are underestimated by as much as 15% and, more dramatically,

Table 1. Summary of the Parameters from Nonlinear Least-Squares Fits of Eqs. (8) to the Lamb-Dip Data Shown in the Bottom Panel of Fig. 4^a

Relative Power	α_{EC}	α_0	S	S Ratio
1.0	1.273(7)	2.43(1)	4.8(1)	1.0
2.0(2)	1.195(3)	2.41(1)	6.7(1)	1.4
3.6(2)	1.148(2)	2.62(1)	10.1(1)	2.1

^aType A standard uncertainties (i.e., 1σ) are given for the least-significant digit, as determined from the least-squares fit.

the α_0 values are $\sim 300\%$ larger than the unsaturated absorption loss rate of 0.811 MHz. A further test of this model is found in the S ratios (see Table 1), which are expected to scale linearly with power according to Eq. (4). The predicted ratios are underestimated by nearly 50% in both cases. We also found that α_0 and S are correlated in the fits and that little change in the standard deviation of the fit results if α_0 is fixed at the average value of 2.49 MHz and only minor ($<10\%$) changes in S are observed. Finally, refitting with a fixed α_{EC} of 1.358 MHz also gives poorly predicted line shapes. From repeated Lamb-dip measurements made at the beginning and end of a 2-h experimental run, systematic drift errors of the baseline are found to be <0.05 MHz and are unlikely to account for even the 15% differences in α_{EC} .

It is at least surprising that with either an increase in the empty-cavity rate or a decrease in the broadband absorption rate toward the values anticipated, the degree of saturation reflected in the Lamb-dip line shapes is predicted at less than what is actually observed. Possible reasons for these exaggerated saturation effects may be found from the following considerations. For example, from simple resonator theory³⁰, changes in the impedance-matching condition can be important under the conditions in our ringdown cell. Perfect impedance matching of the input wave with the resonator is defined when the sum of the cavity mirror losses (exclusive of the input coupler) equals the round-trip cavity losses. In this ideal limit, there would be zero reflective loss from the input coupler and optimum build up of intensity within the resonator ($\times 200$ enhancement for our cavity). However, when on resonance, the round-trip absorption loss of 0.6% is comparable with the output coupler transmission loss of 0.5%. Thus, for constant input intensity, the intracavity enhancement would be expected to decrease from $\times 200$ off resonance to $\times 42$ on resonance, for a change of $>300\%$. It is also well known from this same theory that the ratio of transmitted to intracavity intensity in these two cases is nearly constant ($<0.6\%$ change). For our experiments, the output power leveling scheme enforces this latter condition, thereby circumventing these intracavity intensity changes. It is, however, unavoidable that the cavity Q also decreases as a result of this additional round-trip absorption loss. For example, the empty-cavity linewidth of 216 kHz is predicted to increase to 462 kHz when on resonance (note both widths are larger than the homogeneous

width of 155 kHz for an unsaturated velocity class). It is also likely that the spectral intensity is distributed over this mode prior to each ringdown event as a result of contributions from the 100-kHz frequency modulation scheme used to lock the sideband. With an increase in the spectral bandwidth of light within the cavity, the intensity per unit frequency interval must thereby decrease for a constant intracavity power, decreasing the effect of saturation for a given off-line-center velocity subset. At the center of the Lamb dip, the absorption loss rate decreases owing to a decrease in the population difference. This condition results in a higher cavity Q and an increase in spectral power density and, thus, tends to exaggerate the saturation effect for the zero velocity subset, consistent with the trends observed here. As a further complication, the magnitude of this effect diminishes as the degree of saturation increases and is a consequence of the increase in the power-broadened homogeneous linewidth according to Eq. (7). Finally, we note that Eqs. (8) are derived in the plane-wave limit. Therefore, the effect of saturation integrated over the intensity profile of the TEM₀₀ mode is ignored. The ensemble average of these nonlinear effects will certainly change the Lamb-dip width, depth, and unsaturated absorption coefficient from that predicted by Eqs. (8). Further studies of weaker transitions in ethylene and ozone are currently in progress, where the effects of saturation are expected to be less dominant.

As a final note, it is worth addressing whether the CRDS will be exponential or nonexponential as a result of saturation. The ringdown signal for a saturable absorber is expressed by the following differential equation:

$$dI/dt = -c[\alpha_{EC} + \alpha_0/(1 + I/I_S)]I, \quad (11)$$

where the total losses of the system include a cavity loss term, α_{EC} , and a nonlinear absorption loss term that depends on saturation. To understand whether this equation predicts an exponential or nonexponential function for the intensity decay through the cavity, one must consider the difference between the ringdown time and the population relaxation times and the effect this difference has on the absorption coefficient. For these experiments, the ringdown time (<600 ns) is much shorter than the relaxation times (~10 μ s). This indicates that, during the course of the ringdown decay, the saturated molecules do not relax to the ground state nor are replaced because of molecular motion, and the population difference is unchanged. As a result, the absorption losses are constant at the saturated value as the intensity leaks out of the cavity, and the ringdown decay will be a simple exponential. These are the conditions in our experiment since the ringdown signals measured both on and off the peak of the Lamb Dip absorption fit well to single exponential decays over >3- μ s interval (~6 τ).

In the other limit when ringdown times are long compared with T_1 and T_2 relaxation times, the ab-

sorption losses are not constant, and nonexponential behavior describes the ringdown decay as given by Eq. (11). This nonexponential character arises from the fact that the molecules can now relax on the time scale of the ringdown decay, yielding a time-dependent absorption coefficient.¹⁵ At different times along the ringdown decay, there are different absorption coefficients that are due to the change in the population difference throughout the decay and to the change in the saturation effect as the intensity leaks out of the cavity. At initial times along the ringdown signal, the molecular ensemble will be saturated and the absorption rate will depend on the saturated absorption coefficient. At longer times, an increasing fraction of the molecules will relax to the ground state and the saturation effect will decrease because the intracavity intensity will have decreased from its initial value. As a consequence, the absorption coefficient will asymptotically approach its unsaturated value. These effects have been observed before by Romanini *et al.*¹⁵ The more complete theory of nonlinear CRDS will need to address these issues to gain a complete account of the effects of optical saturation.

5. Conclusions

We have successfully demonstrated the use of cw CRDS to observe Doppler-free nonlinear absorption in a low-pressure sample of C₂H₄ in He by using a low-power (~1-mW) source, and we have been able to quantify the saturation systematically. Strong saturation is observed because of the build up of intensity inside the resonantly pumped ringdown cavity, resulting in a Doppler-free Lamb dip at the center of the Doppler-broadened line. The low power used in the present experiments bodes well for the use of other tunable infrared sources, such as cw optical parametric oscillators or quantum cascade lasers.^{35,36} A key feature, however, is that the source should have a sufficiently narrow bandwidth so that one can efficiently excite a single mode of the ringdown cavity.

The mirrors that we used are of modest reflectivity, compared with those currently available in the mid-infrared.³⁷ However, it should be recognized that, even with the present mirrors, strong saturation is observed when the flux on the detector is only a modest factor (two times) above the detector noise. For the present experiments, a further increase in the reflectivity of the mirrors would likely be counterproductive, as we would have strong saturation even at the lowest output optical intensities required for good signal-to-noise ratio on the detector. This can be overcome by the use of heterodyne detection methods,³⁸ but at a further increase in experimental complexity and bandwidth requirements on the detector. Furthermore, with increased mirror reflectivity, the locking of the cavity mode to the laser becomes more difficult, and increased fluctuations of the initial decay intensity can be expected. Although this is not a limitation for linear absorption CRDS with an ideal linear detector, these fluctuations are clearly unde-

sirable in nonlinear spectroscopy inasmuch as the spectroscopic features being observed are intensity dependent.

A goal of our experiments was to develop a tool for the quantitative study of optical saturation in the mid-infrared. Such an instrument should allow determination of the infrared transition moment of radicals and other unstable species for which the integrated line strength cannot be directly determined from the observed absorption strength that is due to an unknown sample concentration. Once the line strengths have been determined by study of the optical saturation at low pressure, that transition can be used for quantitative determination of the concentration of that particular unstable species. It is advantageous to work at pressures low enough that relaxation is dominated by transit-time broadening, because this can be calculated quantitatively from the TEM₀₀ mode profile in the cavity. Further development along these lines requires a quantitative calculation of the saturated ringdown transients without extraneous assumptions. An important feature to be studied is the degree to which the transients are nonexponential, inasmuch as this will provide a direct measure of the saturation of the optical absorption.

This study was supported by the Petroleum Research Fund, administered by the American Chemical Society. We also acknowledge partial support from the NASA Upper Atmospheric Research Program. Paul Rabinowitz is acknowledged for the use of equipment, and Roger van Zee and Pat Looney are acknowledged for their helpful discussions.

References and Notes

1. K. K. Lehmann and D. Romanini, "The superposition principle and cavity ring-down spectroscopy," *J. Chem. Phys.* **105**, 10,263–10,277 (1996).
2. J. T. Hodges, J. P. Looney, and R. D. van Zee, "Response of a ring-down cavity to an arbitrary excitation," *J. Chem. Phys.* **105**, 10,278–10,288 (1996).
3. P. Zalicki and R. N. Zare, "Cavity ring-down spectroscopy for quantitative absorption measurements," *J. Chem. Phys.* **102**, 2708–2717 (1995).
4. J. P. Looney, J. T. Hodges, and R. D. van Zee, "Quantitative absorption measurements using cavity-ringdown spectroscopy with pulsed lasers," in *Cavity-Ringdown Spectroscopy: an Ultratrace-Absorption Measurement Technique*, K. A. Busch and M. A. Busch, eds. (Oxford University Press, Oxford, UK, 1998), Chap. 7.
5. A. O'Keefe and D. A. G. Deacon, "Cavity ring-down optical spectrometer for absorption measurements using pulsed laser sources," *Rev. Sci. Instrum.* **59**, 2544–2551 (1988).
6. K. J. Schulz and W. R. Simpson, "Frequency-matched cavity ring-down spectroscopy," *Chem. Phys. Lett.* **297**, 523–529 (1998).
7. Y. He, M. Hippler, and M. Quack, "High-resolution cavity ring-down absorption spectroscopy of nitrous oxide and chloroform using a near-infrared cw diode laser," *Chem. Phys. Lett.* **289**, 527–534 (1998).
8. R. Engeln, G. Berden, R. Peeters, and G. Meijer, "Cavity enhanced absorption and cavity enhanced magnetic rotation spectroscopy," *Rev. Sci. Instrum.* **69**, 3763–3769 (1998).
9. D. Romanini, J. Gambogi, and K. K. Lehmann, "Cavity ring down spectroscopy with cw diode laser excitation," in *Proceedings of the 50th International Symposium on Molecular Spectroscopy*, T. A. Miller, ed. (Department of Chemistry, Ohio State University, Columbus, Ohio, 1995), p. 284.
10. D. Romanini, A. A. Kachanov, N. Sadeghi, and F. Stoeckel, "CW cavity ring down spectroscopy," *Chem. Phys. Lett.* **264**, 316–322 (1997).
11. R. Engeln, G. von Helden, G. Berden, and G. Meijer, "Phase shift cavity ring down absorption spectroscopy," *Chem. Phys. Lett.* **262**, 105–109 (1996).
12. D. Romanini, A. A. Kachanov, and F. Stoeckel, "Cavity ring-down spectroscopy: broad band absolute absorption measurements," *Chem. Phys. Lett.* **270**, 546–550 (1997).
13. B. A. Paldus, C. C. Harb, T. G. Spence, B. Wilke, J. Xie, J. S. Harris, and R. N. Zare, "Cavity-locked ring-down spectroscopy," *J. Appl. Phys.* **83**, 3991–3997 (1998).
14. D. Romanini, A. A. Kachanov, and F. Stoeckel, "Diode laser cavity ring down spectroscopy," *Chem. Phys. Lett.* **270**, 538–545 (1997).
15. D. Romanini, P. Dupre, and R. Jost, "Non-linear effects by cw cavity ring-down spectroscopy in jet-cooled NO₂," *Vib. Spectrosc.* **19**, 93–106 (1999).
16. J. J. Scherer, D. Voelkel, D. J. Rakestraw, J. B. Paul, C. P. Collier, R. J. Saykally, and A. O'Keefe, "Infrared Cavity Ring-down Laser-Absorption Spectroscopy (IR-CRLAS)," *Chem. Phys. Lett.* **245**, 273–280 (1995).
17. R. Engeln, E. van den Berg, G. Meijer, L. Lin, G. M. H. Knipfels, and A. F. G. van der Meer, "Cavity ring down spectroscopy with a free-electron laser," *Chem. Phys. Lett.* **269**, 293–297 (1997).
18. E. R. Crosson, P. Haar, G. A. Marcus, H. A. Schwettman, B. A. Paldus, T. G. Spence, and R. N. Zare, "Pulse-stacked cavity ring-down spectroscopy," *Rev. Sci. Instrum.* **70**, 4–10 (1999).
19. M. Muertz, B. Frech, and W. Urban, "High-resolution cavity leak-out absorption spectroscopy in the 10 mm region," *Appl. Phys. B* **69**, 243–249 (1999).
20. G. Magerl, W. Schupita, and E. Bonek, "A tunable CO₂ laser sideband spectrometer," *IEEE J. Quantum Electron.* **QE-18**, 1214–1219 (1982).
21. SPST p-i-n Diode Switch, Series SW-2184-1A, American Microwave Corporation, 7311G Grove Rd., Frederick, Md. 21701.
22. II-VI, Inc., 375 Saxonburg Blvd., Saxonburg, Pa. 16056.
23. K. M. Evenson, C. C. Chou, B. W. Bach, and K. G. Bach, "New cw CO₂ laser lines: the 9- μ m hot band," *IEEE J. Quantum Electron.* **30**, 1187–1188 (1994).
24. E. Riedle, S. H. Ashworth, J. T. Farrell, Jr., and D. J. Nesbitt, "Stabilization and precise calibration of a continuous-wave difference frequency spectrometer by use of a simple transfer cavity," *Rev. Sci. Instrum.* **65**, 42–48 (1994).
25. R. D. van Zee, J. T. Hodges, and J. P. Looney, "Pulsed, single-mode cavity ring-down spectroscopy," *Appl. Opt.* **38**, 3951–3960 (1999).
26. D. C. Reuter and J. M. Sirota, "Absolute intensities and foreign gas broadening coefficients of the 11_{1,10} \leftarrow 11_{2,10} and 18_{0,18} \leftarrow 18_{1,18} lines in the ν_7 band of C₂H₄," *J. Quant. Spectrosc. Radiat. Transfer* **50**, 477–482 (1993).
27. E. Giacobino, M. Devaud, F. Biraben, and G. Grynberg, "Doppler-free two-photon dispersion and optical bistability in rubidium vapor," *Phys. Rev. Lett.* **45**, 434–437 (1980).
28. F. T. Arecchi and A. Politi, "Optical bistability in a resonant two-photon absorber," *Lett. Nuovo Cimento* **23**, 65–69 (1978).
29. A. T. Rosenberger, L. A. Orozco, H. J. Kimble, and P. D. Drummond, "Absorptive optical bistability in two-state atoms," *Phys. Rev. A* **43**, 6284–6302 (1991).
30. A. E. Siegman, *Lasers* (University Science, Mill Valley, Calif., 1986), Chap. 24.

31. V. S. Letokhov and V. P. Chebotayev, *Nonlinear Laser Spectroscopy* (Springer-Verlag, New York, 1977), p. 57.
32. W. Demtroder, *Laser Spectroscopy: Basic Concepts and Instrumentation*, 2nd ed. (Springer-Verlag, New York, 1996), p. 443.
33. C. J. Borde, J. L. Hall, C. V. Kunasz, and D. G. Hummer, "Saturated absorption line shape: calculation of the transit-time broadening by perturbation approach," *Phys. Rev. A* **14**, 236-244 (1976).
34. V. S. Letokhov, *High-Resolution Laser Spectroscopy*, K. Shimoda, ed. (Springer-Verlag, New York, 1976), p. 99.
35. J. Faist, F. Capasso, C. Sirtori, D. L. Sivco, J. N. Baillargeon, S.-N.G. Chu, and A. Y. Cho, "High power mid-infrared quantum cascade lasers operating above room temperature," *Appl. Phys. Lett.* **68**, 3680-3682 (1996).
36. R. Q. Yang, B. H. Yang, D. Zhang, C.-H. Lin, S. J. Murry, H. Wu, and S. S. Pei, "High power mid-infrared interband cascade lasers based on type-II quantum wells," *Appl. Phys. Lett.* **71**, 3400-3402 (1997).
37. R. Nubling, Laser Power Optics, Inc., San Diego, Calif. (personal communication, 1999).
38. M. D. Levenson, B. A. Paldus, T. G. Spence, C. C. Harb, J. S. Harris, Jr., and R. N. Zare, "Optical heterodyne detection in cavity ring-down spectroscopy," *Chem. Phys. Lett.* **290**, 335-340 (1998).